Journal of
Ship&Ocean
Technology
©DECEMBER 2001

SOTECH Vol. 5, No. 4, pp. 29~43, 2001

Numerical Simulation of Breaking Waves around a Two- Dimensional Rectangular Cylinder Piercing Free Surface

Seung-Nam Kim[1] and Young-Gill Lee[2]

[1]Department of Naval Architecture, Graduate School of Inha University, Younghyun-Dong, Nam-gu, Incheon, Korea

[2]Department of Naval Architecture and Ocean Engineering, Inha University, Younghyun-Dong, Nam-gu, Incheon, Korea; E-mail: younglee@inha.ac.kr

Abstract

In this paper, free surface flows around an advancing two-dimensional rectangular cylinder piercing the free surface are studied using numerical and experimental methods. Especially, wave breaking phenomenon around the cylinder is treated in detail. A series of numerical simulations and experiments were performed for the purpose of comparison.

For the numerical simulations, a finite difference method was adopted with a rectangular grid system, and the variation of the free surface was computed by the marker density method. The computational results are compared with the experiments. It is confirmed that the present numerical method is useful for the numerical simulation of nonlinear free surface waves around a piercing body.

Keywords: free surface, breaking waves, two-dimensional rectangular cylinder, two-layer flow, marker density

1 Introduction

Concerned in this paper is the wave breaking which is a phenomenon of flow separation of turbulence, which is not necessarily isotropic, and of the two-phase flow including air-bubble. Since the breaking of free surface waves often causes significant wave forces on structures, the understanding of the phenomena is very important in the field of naval architecture and ocean engineering.

Many classical theories have been very useful for understanding free surface waves and for the estimation of the resultant wave forces. However, it ceases to be useful when the above-mentioned wave breaking plays a significant role, since classical theories are generally based on linear assumptions. Due to the rapid development of computers, various numerical methods for viscous rotational flows have been devised based on the MAC(Marker And Cell) method(Welch et al 1966). Chan and Street(1970) and Hirt and Nichols(1981) modified the original MAC method for the refined satisfaction of the dynamic and kinematic free surface boundary conditions. Before the VOF(Volume Of Fluid) method was introduced, earlier numerical techniques to define

the location of free surface could hardly treat with the large distortion of the free surface. The VOF method overcame the drawback by allowing steep and multi-valued interface involved with breaking and merging. However, even in that method the free surface could not be sharply defined. The boundary element method has been used as one of the effective tools for the free surface wave problems. Some important works(Longuet-Higgins and Cokelet 1976, Greenhow et al 1982) with this method have significantly contributed to the better understanding of the mechanism of wave breaking phenomena. However, these works lose their validity when the overturning wave front impinges on the free surface beneath the wave fore-front and succeeding complicated motions become more important. The versatile applicability of the finite difference method in the field of free surface waves was demonstrated by Harlow and Amsden(1971). However, the details of the method, especially the technique of the implement of free surface conditions, were not well described. Miyata et al.(1986) simulated breaking waves for a submerged circular cylinder under the free surface in waves by using a finite difference method called TUMMAC-Vbk. However, this method also loses its validity when it is continuously executed to simulate the flow phenomena after the wave breaking which includes air-trapping. Many other techniques, such as SPH(Monaghan 1994), marker density technique(Park and Miyata 1994) and level set method(Sussman 1994) have been developed to simulate sharp and large moving boundary deformation with wave breaking phenomena.

The computation of the deformation of solitary waves on a sloping beach was performed using SUMMAC(Chan and Street 1970) and VOF method(Wang and Su 1993). Hino et al.(1984) and Monaghan(1994) simulated the deformation of periodic waves on a beach using TUMMAC and SPH, respectively. Heo and Lee(1996) simulated breaking waves on various beach slopes using a hybrid method, which is a combination of the line segment method and the marker method. Kim and Lee(2001) simulated breaking waves on a circular cylinder using the marker-density method.

In this paper, various numerical techniques to treat the kinematic free surface boundary condition were briefly summarized and compared before the computation of the breaking waves. Breaking waves around an advancing rectangular cylinder are numerically simulated. Waves are generated in front of the advancing rectangular cylinder, and advance faster than the cylinder. The waves are gradually steepened, then are broken. The marker density method is adopted for the computation of the free surface waves after the breaking. For various conditions, computation and experiments were performed for the purpose of comparison.

2 Computational method

2.1 Governing equations

The governing equations for the present computations are the following Navier-Stokes equations and the continuity equation of two-dimensional incompressible viscous flow.

$$\frac{\partial u}{\partial t} + u\frac{\partial u}{\partial x} + w\frac{\partial u}{\partial z} = -\frac{1}{\rho}\frac{\partial p}{\partial x} + \frac{\mu}{\rho}\left(\frac{\partial^2 u}{\partial x^2} + \frac{\partial^2 u}{\partial z^2}\right) \tag{1}$$

$$\frac{\partial w}{\partial t} + u\frac{\partial w}{\partial x} + w\frac{\partial w}{\partial z} = -\frac{1}{\rho}\frac{\partial p}{\partial z} + \frac{\mu}{\rho}\left(\frac{\partial^2 w}{\partial x^2} + \frac{\partial^2 w}{\partial z^2}\right) + g \tag{2}$$

$$\frac{\partial u}{\partial x} + \frac{\partial w}{\partial z} = 0 \tag{3}$$

where u and w are the velocity components in the x and z direction, respectively. μ is the dynamic viscosity coefficient, ρ is the density, and g is the gravitational acceleration. During the computation of two-phase flow, densities of the water and the air are assumed constant.

2.2 Finite difference method

The governing equations are discretized by using finite differencing schemes in a fixed staggered variable mesh system. The Adams-Bashforth scheme is adopted for the time derivative terms in momentum equations. Approximating convection terms, we need a third order upstream scheme, a second order hybrid scheme and a first order upstream scheme depending upon the number of neighboring fluid cells. The other spatial derivative terms are discretized by using the centered differentiating scheme. Pressure distribution is obtained by solving the Poisson equation of pressure and the SOR(Successive Over Relaxation) method is employed to solve the finite difference version of this equation.

2.3 Body and free surface boundary conditions

No-slip condition is implemented with irregular leg length for the calculation of differential terms around the body surface and flux calculation for divergence zero in a body boundary cell which is involving the body surface. In each body boundary cell, the velocity and pressure are computed by a simultaneous iteration method until the pressure is converged. Refer to references 16 and 18 regarding the details of the body boundary conditions.

The dynamic free surface boundary condition is as follows.

$$p = p_0 \qquad \text{on free surface} \tag{4}$$

where p_0 is the atmospheric pressure.

The kinematic free surface boundary condition is as follows.

$$\frac{D(z-\eta)}{Dt} = 0 \qquad \text{on free surface} \tag{5}$$

where η is the wave elevation. Refer to reference 17 regarding the details of the free surface boundary conditions.

2.3.1 Marker density method

When we use the marker and line-segment methods, it is not easy to treat the free surface motions of the nonlinear character after the wave breaking. Therefore, the marker density method is adopted in the present computation for the satisfaction of the kinematic free surface boundary condition with wave breaking.

2.3.2 Position of free surface

The following transport equation of the density function is employed for the determination of the location of the free surface instead of Equation (5).

$$\frac{\partial M_\rho}{\partial t} + u\frac{\partial M_\rho}{\partial x} + w\frac{\partial M_\rho}{\partial z} = 0 \tag{6}$$

The location of the interface between two fluid regions is determined by the following definition of the free surface with the density function.

$$M_\rho = \widetilde{M_\rho} = \frac{\rho^{<1>} + \rho^{<2>}}{2} \qquad \text{on the interface} \tag{7}$$

2.3.3 Extrapolation of physical quantity near body Surface

The computation of density function is very difficult in the place where the free surface meets the body surface. Therefore, the density function value here is determined by extrapolating the density function value from an adjacent cell to the interface. In fact, the density function value on the interface is decided using equivalent extrapolation in the horizontal direction as shown in (8). Figure 1 is the schematic sketch of marker density extrapolation near the free surface.

$$\begin{aligned} M_{\rho(i+1,k)} &= M_{\rho(i,k)} \\ M_{\rho(i-1,k)} &= M_{\rho(i,k)} \end{aligned} \tag{8}$$

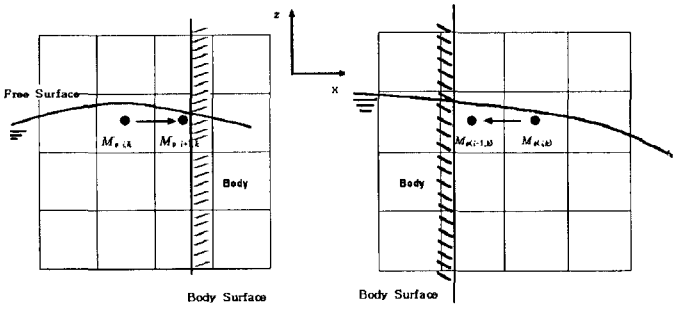

Figure 1: Schematic sketch of the marker-density extrapolation near the free surface

2.4 Computational conditions

In the present investigation, the computations are performed for the cases with the following conditions. The breadth of the rectangular cylinder is 0.2m, its height is 0.225m, and its submerged depth is 0.1m. The submerged depth is defined as the distance from the bottom of the rectangular cylinder to the free surface of calm water. Stokes' waves propagating from left to right and uniform flows are generated by specifying appropriate boundary conditions for u,w at the inflow boundary. The detailed computational conditions are shown in Table 1 and Table 2. The computational domain is shown in Figure 2. The length and depth of the domain are 3.0m and 1.6m, respectively.

Table 1: Computational condition for a rectangular cylinder piercing free-surface in waves

Wave Length(m)	1.0	
Wave Height(m)	0.02	0.04
Inflow B.C.	Stokes	Stokes
dxmin(m)	0.0085	0.0085
dzmin(m)	0.0035	0.0035
dt(sec)	0.001	0.001
Computational domain(m)	2.5*1.6	

In the case of the incident wave, predicting the occurrence of wave breaking and according to occurrence or not, it has been divided into two circumstances. Actual calculation done on each circumstance is as follows. The wave length is 1.0m, the wave amplitudes are 0.02m and 0.04m, and the period is 1.003sec. The minimum size of mesh is 0.0085m in x direction and 0.0035m in z direction as shown in Table 1. Stokes' equations are used for the generation of numerical waves on the inflow boundary as follows.

$$\begin{aligned} u &= c\left[a\omega\frac{\cosh(z+d)}{\sin kd}\cos\theta + \frac{3}{4}(aw)^2\frac{\cosh 2(z+d)}{\sin^4 kd}\cos 2\theta\right] \\ w &= c\left[a\omega\frac{\sinh(z+d)}{\sin kd}\sin\theta + \frac{3}{4}(aw)^2\frac{\sinh 2(z+d)}{\sin^4 kd}\sin 2\theta\right] \end{aligned} \tag{9}$$

where a, k, d, $\omega$and c are the wave height, wave number, water depth, wave frequency and wave celerity, respectively.

In the case of the uniform flow, Froude numbers based on period are 0.5(u=0.496m/s), 0.75(u=0.742m 1.0(u=0.990m/s) and 1.25(u=1.237m/s). The minimum sizes of mesh are from 0.0065 to 0.0085 in x direction and 0.0035 in z direction as shown in Table 2.

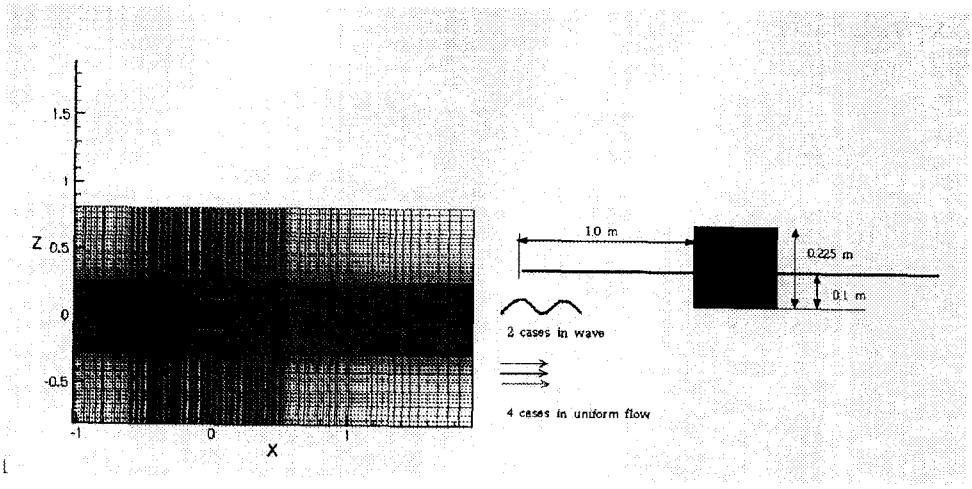

Figure 2: Computational domain and computational conditions

Table 2: Computational condition for a rectangular cylinder piercing the free-surface in uniform flows

Fn	0.5	0.75	1.0	1.25
Inflow B.C.	Uniform Flow			
dxmin(m)	0.0085	0.0065	0.0065	0.0085
dxmin(m)	0.0035			
dt(sec)	0.001	0.0002	0.0002	0.0002
Computational domain(m)	4.0*1.6	2.5*1.6		

3 Description of experiments

The experiments were carried out in the towing tank of Inha University. The length, width and water depth of the towing tank are 80m, 5m and 2.7m, respectively. A rectangular channel with two side walls made of transparent acrylic plastic plate with sharp leading and trailing edges is used for generating a two-dimensional flow field. The length, height and thickness are 1.6m, 0.625m and 10mm, respectively. Then, a rectangular piercing cylinder which is also made of transparent acrylic plastic plate is exactly fit in across two side walls of the channel. The length, breadth, height and thickness are 1.0m, 0.2m, 0.225m and 10mm, respectively. Two circular holes with a diameter of 10mm each are drilled at the top and bottom ends which let water in and out of the cylinder and thereby neutralize the buoyancy effect.

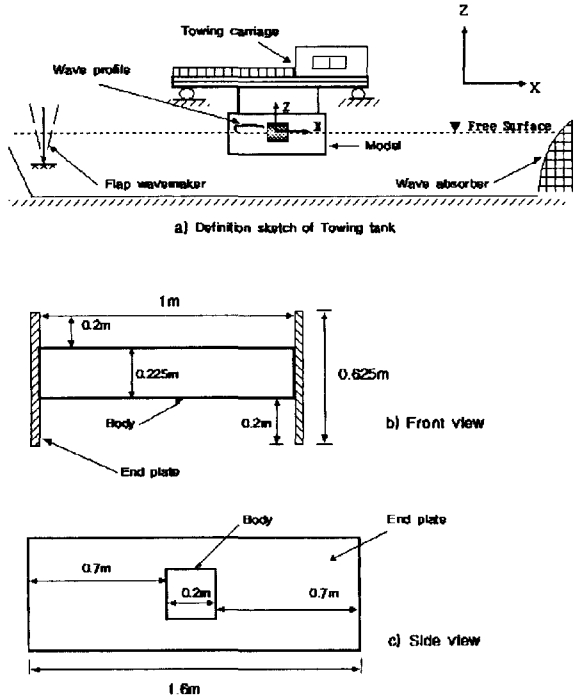

Figure 3: Experimental setup of model and towing tank

The depth of submergence is 0.1m. The mesh size used in the experiment was decided within the range that satisfies the accuracy level of calculation predicting the amplitude of the wave that will be simulated and wave height around a substance. The size is 0.02m. The towing carriage and the channel are driven with speeds set in advance which are usually expressed as Froude number based on the submerged depth. In the present experiment, the Froude numbers are 0.5, 0.75, 1.0, 1.25 and 1.5, respectively. Figure 3 shows the experimental setup consisting of the model and the towing tank.

The measurement of wave elevations along the longitudinal line of the rectangular channel was carried out using the wave height gage of servo needle type. For the purpose of easy photographing and measuring the wave profiles and patterns, horizontal and vertical lines with intervals of 2.0cm were marked on the surface of the transparent acrylic plastic plate of the channel. The photography of the wave patterns was done by a digital video camera.

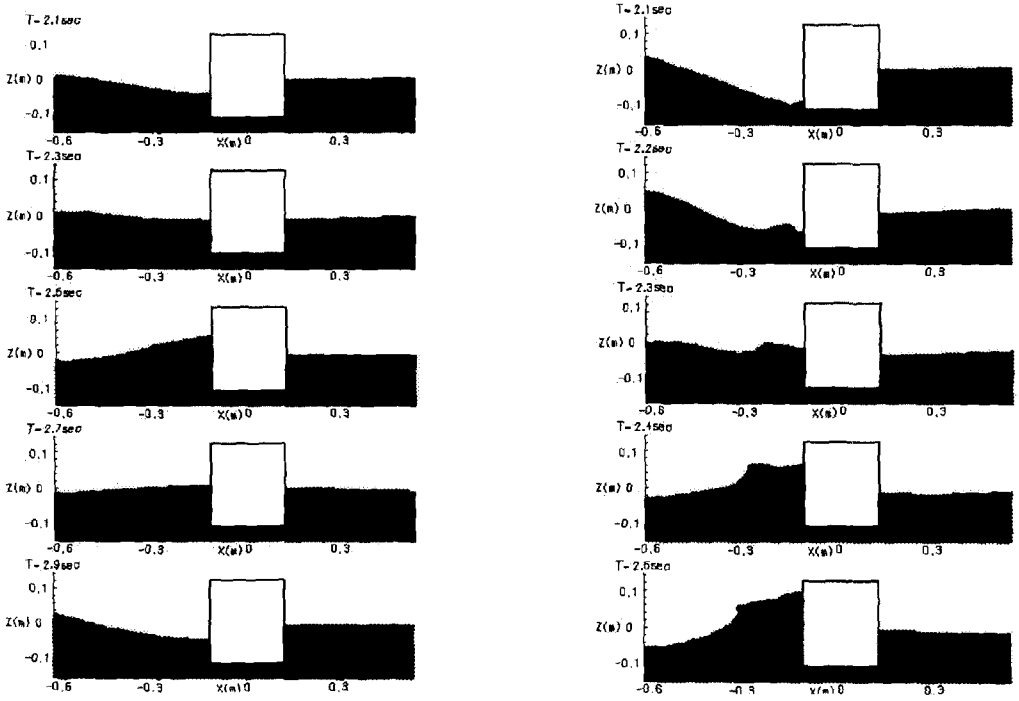

(a) (λ:1.0m, h_0:0.02m) (b) (λ:1.0m, h_0:0.04m)

Figure 4: Free surface profiles from the numerical simulation in waves

4 Results of computation and discussions

4.1 A rectangular cylinder in waves

The time-sequence of wave profiles, which is numerically simulated for a rectangular cylinder in waves, shown in Figure 6, illustrate a comparison between the case without breaking phenomena

and the case with breaking phenomena on the free surface. In this figure, the time intervals are 0.2 sec and 0.1 sec, and the amplitude of the right-hand side case (wave height is 0.04m.) is larger than the left-hand side case (wave height is 0.02m.), because an appropriate steep wave is used in the present study for the simulation of a typical overturning breaker. In the first figure (T=2.1sec) of each case in Figure 4, the front of the wave generated by the numerical wave-maker is approaching the rectangular cylinder. Here, T is the time. The time-sequence of wave profiles for the low amplitude wave is similar to the periodic inflow wave profiles. In the case of the high amplitude wave, the free surface is deformed into a jump-like configuration in front of the cylinder as shown in the third and fourth stages in the right-hand side of Figure 4. After that, it breaks in front of the cylinder, and the wave breaking phenomena are observed in the fifth stage successively. Therefore, the sequence of wave breaking (steepening of wave-surface→singularity of wave surface→overturning or spilling) is representatively well observed in this figure.

4.2 A rectangular cylinder in uniform flows

To verify usefulness of the simulation, the numerical & experimental profiles of the free surface have been compared. The figures from Figure 5 to Figure 16 show comparisons of chronologically occurred wave profiles and its heights that were produced by experiments and numerical simulations under the condition of incident velocity at its range from Fn 0.5 to 1.25. However, areas of experiments and numerical simulations have been confined to the space around rectangular cylinder due to constraints in them. Wave characteristics and its profiles created by the rectangular cylinder have varied with incident velocity.

When Fn=0.5, a cyclically created wave has occurred in front of the cylinder. Figure 5 shows the changing profiles of the free surface around the cylinder as the observed time elapses. Additionally, in the front wave that occurred in front of the rectangular cylinder is indicated with the bold lines for easy discernment. Waves occurring cyclically in front of the rectangular cylinder located in uniform flow have moved forward. Figure 6 shows wave profiles calculated by the numerical simulation, and it shows the similar behavior seen in the experiments. Figure 7 shows a comparison of the time averaged wave height taken through the experiment and numerical simulation. According to this, values in front of the cylinder show consistent pattern, but those at the rear of it show very different results. Although this is a low inflow speed condition, behind the rectangular cylinder, there was difficulty in the simulation of free surface because of the unsteady flow characteristic of the flow and its complexity. And, the difference between the results of numerical simulation and experiment was large because of the inaccuracy of the measurement since the absolute value of the measurement of the experiment was small.

When Fn=0.75, a cyclical wave has occurred as it also has at Fn 0.5. Figure 8 presents profiles of free surface in the experiment. As indicated in the above observation, the wave occurring cyclically in front of the rectangular cylinder located in uniform flow has moved forward. Figure 9, wave profiles in numerical simulation, identify the result of the experiment. Figure 10 shows comparison of the averaged time to wave height as Figure 7. According to this, values in front of the cylinder show somewhat of a consistent pattern, but those at the rear of it also show very different results. Similar to Fn=0.5, this also is a comparatively low inflow speed which wave does not occur. However, because of the characteristic of the unsteady flow and from the occurrence of a more complex flux from increase of speed (compared to the case of Fn=0.5), difference was seen in the result of simulation and experiment.

Figure 5: Photographs of free surface waves (Fn=0.5)

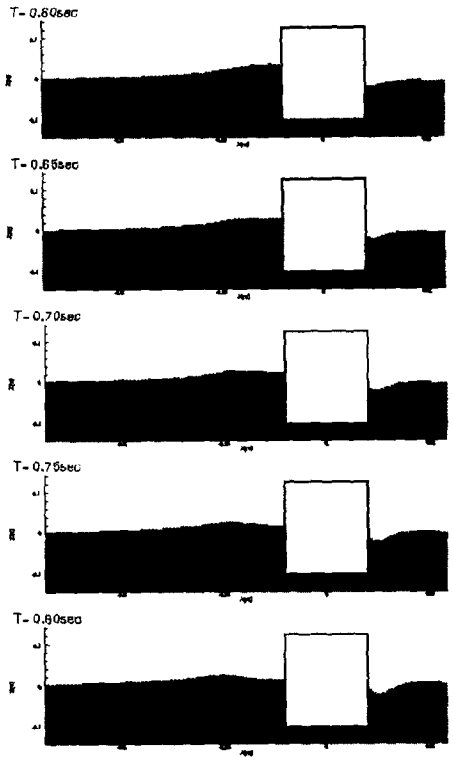

Figure 6: Free surface profiles from the numerical simulation in uniform flow (Fn=0.5)

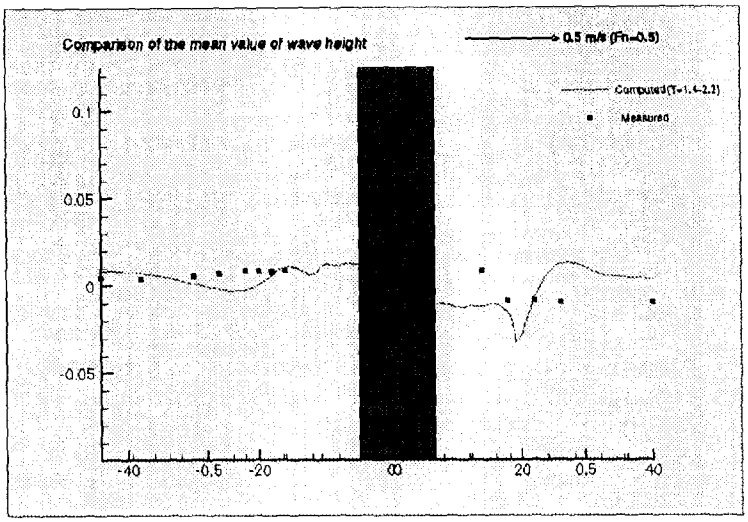

Figure 7: Comparison of the time mean values of wave height (Fn=0.5)

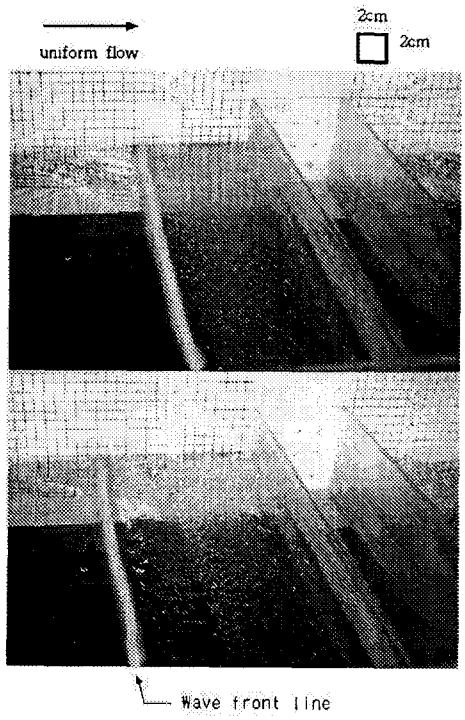

Figure 8: Photographs of free surface waves (Fn=0.75)

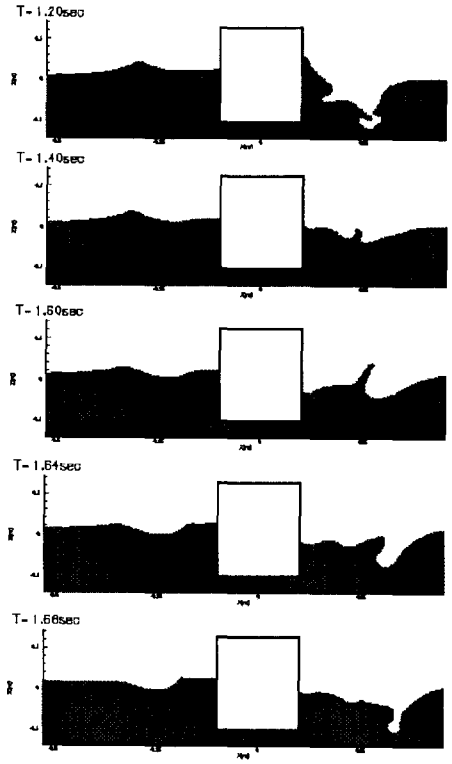

Figure 9: Free surface profiles from the numerical simulation in uniform flow (Fn=0.75)

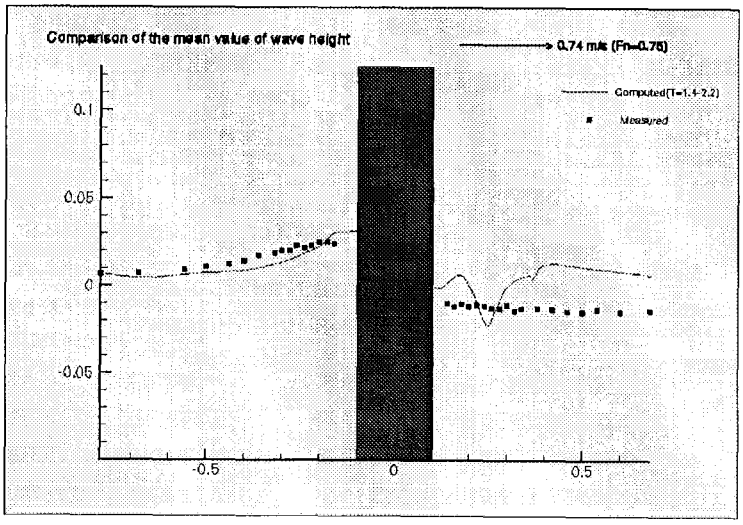

Figure 10: Comparison of the time mean values of wave height (Fn=0.75)

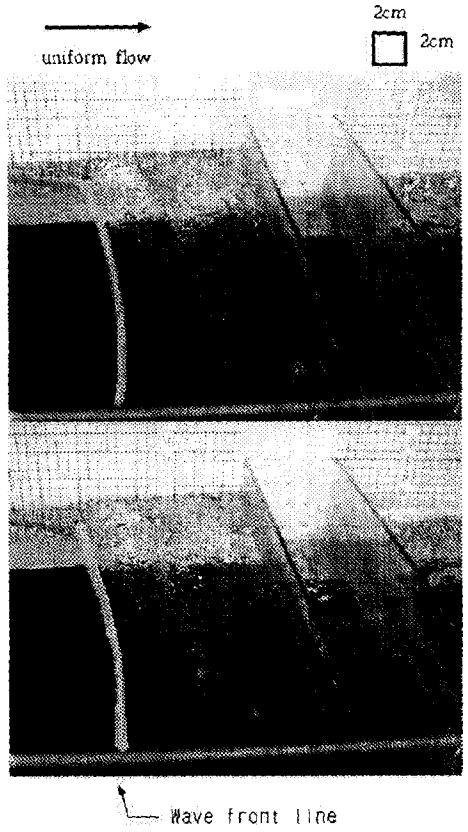

Figure 11: Photographs of free surface waves (Fn=1.0)

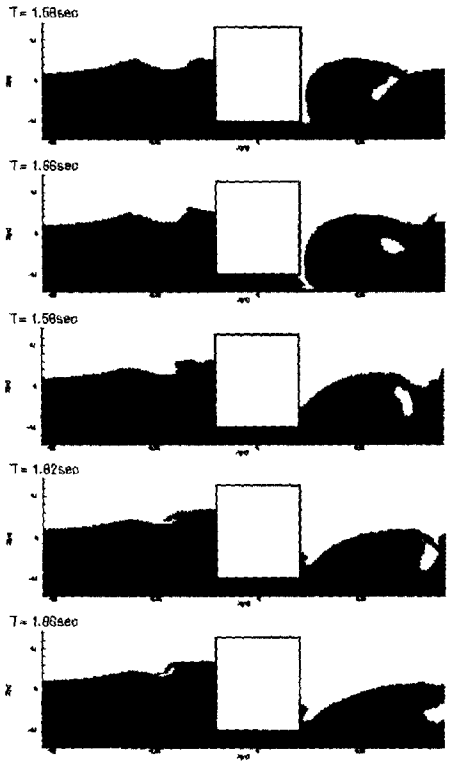

Figure 12: Free surface profiles from the numerical simulation in uniform flow (Fn=1.0)

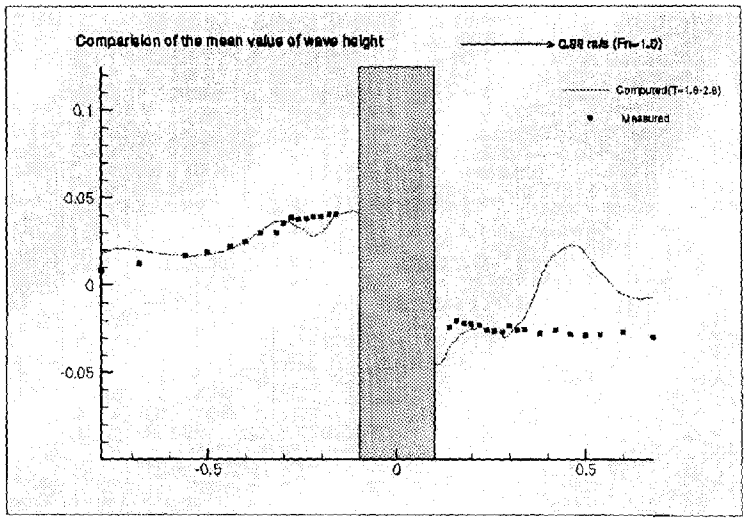

Figure 13: Comparison of the time mean values of wave height (Fn=1.0)

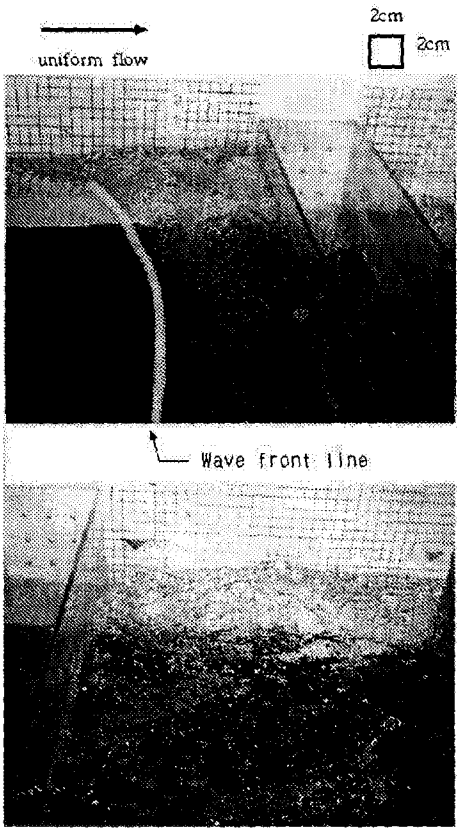

Figure 14: Photographs of free surface waves (Fn=1.25)

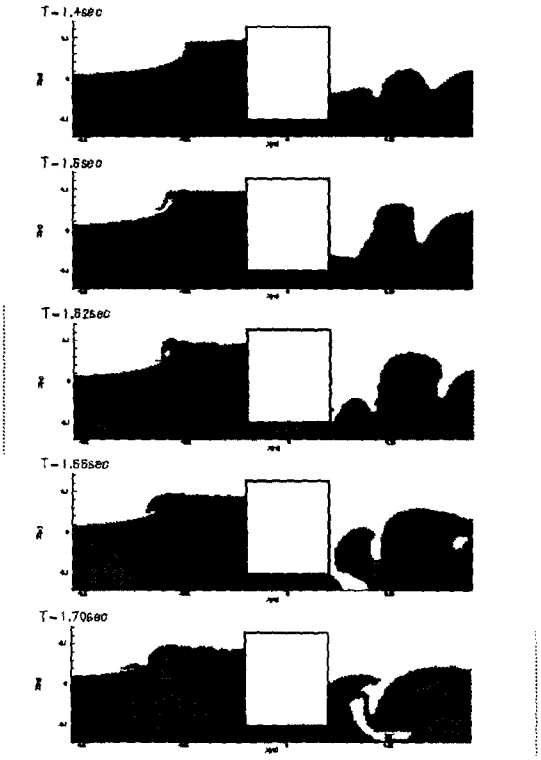

Figure 15: Free surface profiles from the numerical simulation in uniform flow (Fn=1.25)

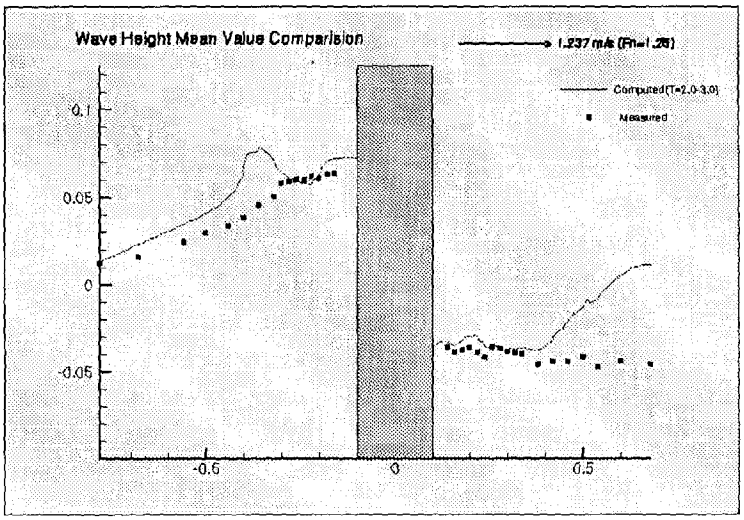

Figure 16: Comparison of the time mean values of wave height (Fn=1.25)

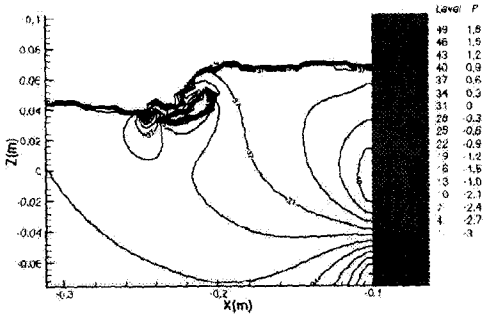

Figure 17: Pressure Contours (Fn=1.0)

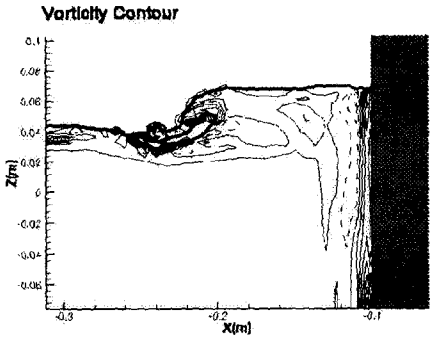

Figure 18: Vorticity Contours (Fn=1.0)

When Fn=1.0, the cyclical wave breaking phenomenon has appeared as different as the above results. Figure 11 presents profiles of free surface in experiment. Although it is in accordance with the above observation that the cyclically occurred wave in front of cylinder has moved forward, spilling type of wave breaking has occurred at the points of 30 40cm distant from the center. Figure 12 shows wave profiles in numerical simulation. In this, the wave breaking phenomenon as in experiment cannot only be observed, but the spilling type of wave breaking can be also observed. In addition to this, the cyclical pattern of spilling-typed wave breaking (steeping of wave-surface→singularity of wave-surface→spilling→impinging→air-trapping) can be observed in detail. Figure 13 shows the comparison of the heights of waves. It was verified that the numerical values from the result of simulation and experiment in front of the cylinder were almost similar. However, behind the cylinder, because of the characteristic of the unsteady flow and from the complexity of the flow, again, it was confirmed that the two results showed a difference. However, that difference was smaller compared to the case of Fn=0.5 and 0.75, that are slower speeds than the present speed. Because of faster inflow speed, this is thought as resulting from the occurrence of waves with longer cycles and relatively large absolute value of measurement.

When Fn=1.25, the cyclical wave breaking phenomenon has also occurred. Figure 14 displays profiles of free surface in the experiment. In this, the cyclical wave has also occurred in front of the cylinder as above, but the plunging type of wave breaking phenomenon has occurred in front of it. Figure 15 displays wave profiles in numerical simulation. According to this, the wave breaking phenomenon as in experiment has occurred, plus cyclical pattern of plunging-typed wave breaking phenomenon can be observed in detail (steeping of wave-surface→singularity of wave surface→overturning→impinging→air-trapping & splashing). Figure 16 presents comparison of the averaged wave heights. Values in front of cylinder are largely consistent, while those in the wave breaking area at a 25 35cm distance forward from the center display with the difference owing to the complicated wave breaking phenomenon. It is shown that values at the rear of cylinder are somewhat in accordance with those in close around the center. It is thought because problems in numerical simulation prevent from comparing results out of experiments over a long period. As discussed above, from the experiment and numerical simulation on rectangular cylinder located in the free surface, in the case of complicated flow, where the phenomenon of wave breaking occurs, there is usefulness of simulations.

When Fn=1.0, the pressure and the vorticity contours by numerical computation are shown in

Figures 17 and 18. These figures illustrate the nonlinear phenomena of the free surface after the wave breaking of a nearly spilling type. After the wave breaking, the high pressure and vorticity are well simulated in these figures.

5 Conclusion

As shown in the present work, the numerical simulation using the marker density method shows good results which are close to the physical phenomena for the wave breaking around an advancing rectangular cylinder. Furthermore, wave elevations are simulated with qualitatively fine results, and from the comparison of time-mean values with experimental results, the present method seems useful for the simulation of complicated nonlinear waves on the free surface. The following conclusions are made from this study.

(1) The nonlinear wave breaking on the free surface is well simulated around a two-dimensional rectangular cylinder. The computed waves in front of the cylinder are in positive agreement with the experimental results.

(2) It is confirmed that the marker density method is very useful for the numerical simulation of complex nonlinear free surface phenomena.

(3) By using the marker density method, the wave breaking procedure could be continuously simulated after the reattachment of the free surface.

(4) The present method is expected to be useful for the simulation of complicated flows in the field of ocean structure involved with the wave breaking phenomena. In the future, further research in the present method is necessary for the introduction of the model of turbulence and free surface impact, and more accurate treatment of the free surface and body boundary conditions.

Acknowledgements

The present work is financed by the Inha University in 1999 and also partly supported by the Research Institute of Marine Systems Engineering, College of Engineering in Seoul National University.

References

CHAN, R.K.C. AND STREET, R.L. 1970 SUMMAC-A Numerical Model for Water Waves. Dept. of Civil Engineering, Stanford University, Stanford, CA, Technical Report No. 135

GREENHOW, M., VINJE, T., BREVIG, P. AND TAYLOR, T. 1982 A Theoretical and Experimental Study of the Capsize of Salter's Duck in Extreme Waves. J. of Fluid Mech., **118**, pp. 221-239

HARLOW, F.H. AND AMSDEN, A.A. 1971 Fluid dynamics. Los Alamos Scientific Lab. Report LA-4700, Los Alamos, New Mexico

HEO, J.K. AND LEE, Y.G. 1996 A Numerical Simulation of Two-dimensional Nonlinear Waves in Surf Zone. Proc. KOJAM '96

HINO, T., MIYATA, H., KAJITANI, H., AND KANAI, M. 1984 A Numerical Solution Method for Nonlinear Shallow Water Waves (Second Report). J. of Soc. Naval Arch. Japan, **154**, pp. 29-39

HIRT, C.W. AND NICHOLS, B.D. 1981 Volume of Fluid(VOF) Method for the Dynamics of free Boundaries. J. of Comput. Physics, **39**, pp. 201-205

INOUE, R. AND KYOZUKA, Y. 1984 On the Nonlinear Wave Forces Acting on Submerged Cylinders. J. of Soc. Nav. Archit. Japan. **156**, pp. 115-117

KIM, S.N. AND LEE, Y.G. 2001 Numerical Simulations of Breaking Waves above a Two-Dimensional Submerged Circular Cylinder. SOTECH, **5**, **3**

LEE, Y.G. AND MIYATA, H. 1990 A Finite Simulation Method for 2D Flows about Bodies of Arbitrary Configuration. J. of The Society of Naval Architects of Japan, **167**, pp. 1-8

LONGUET-HIGGINS, M.S. AND COKELET, E.D. 1976 The Deformation of Steep Surface Waves on Water. Proc. Roy. Soc. London A350, pp. 1-26

MIYATA, H. 1986 Finite-Difference Simulation of Breaking Waves. J. of Comput. Physics **65**, pp. 179-214

MIYATA, H., KAJITANI, H., ZHU, M., KAWANO, T., AND TAKAI, M. 1988 Numerical Study of Some Wave-Breaking Problems by a Finite -Difference Method. J. of Kansai Soc. N.A., Japan. **207**, pp. 11-23

MIYATA, H. AND LEE, Y.G. 1990 Vortex Motions about a Horizontal Cylinder in Waves. Ocean Engineering, **17**, **3**, pp. 279-305

MONAGHAN, J.J. 1994 Simulating Free Surface Flows with SPH. J. of Comput. Physics, **110**

PARK, J.C. AND MIYATA, H. 1994 Numerical Simulation of 2D and 3D Breaking Waves by Finite-Difference Method. J. of Soc. Naval Arch. Japan, **175**, pp. 11-24

SUSSMAN, M. 1994 A Level Set Approach for Computing Solutions to Incompressible Two-phase Flow. J. of Comput. Phys. **114**, pp. 146-159

WANG, Y. AND SU, T.C. 1993 Computation of Wave Breaking on Sloping Beach by VOF Method. Proc. the Third ISOPE, pp. 96-101

WELCH, J.E., SHANNON, J.P. AND DALY, B.J. 1966 The MAC Method. Los Alamos Scientific Lab. Report LA-3425, Los Alamos, N.M.